

## **Electronic Supplementary Information**

for the manuscript entitled

### **Carbon-sulphur cross coupling reactions catalyzed by nickel-based coordination polymers based on metalloligands**

Gulshan Kumar, Firasat Hussain and Rajeev Gupta\*

Department of Chemistry, University of Delhi, Delhi – 110 007 (India)

Fax: +91-11-2766 6605; E-mail: [rgupta@chemistry.du.ac.in](mailto:rgupta@chemistry.du.ac.in)

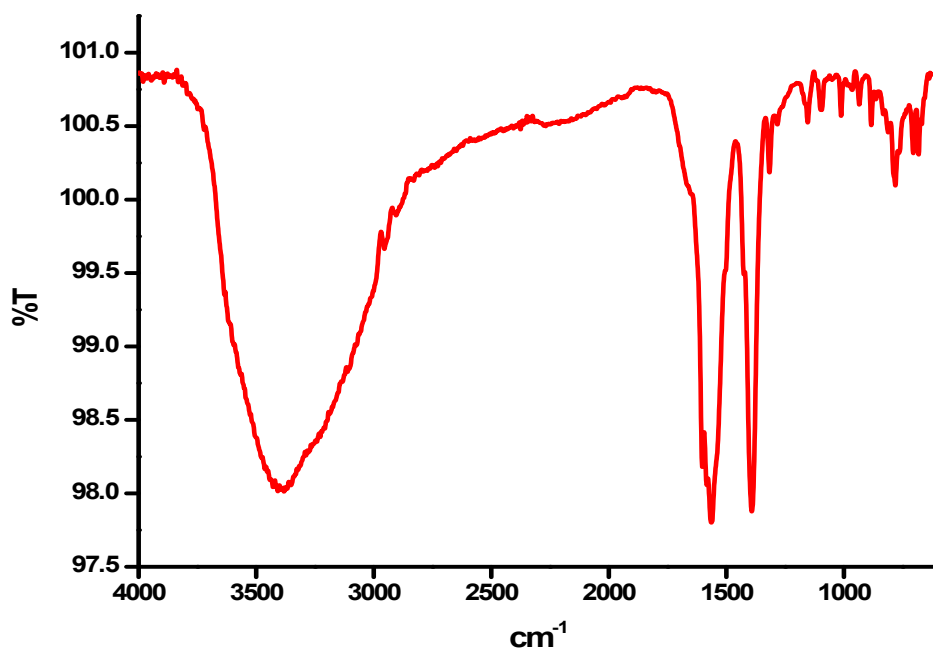


Figure S1. FTIR spectrum of **1-Ni**.

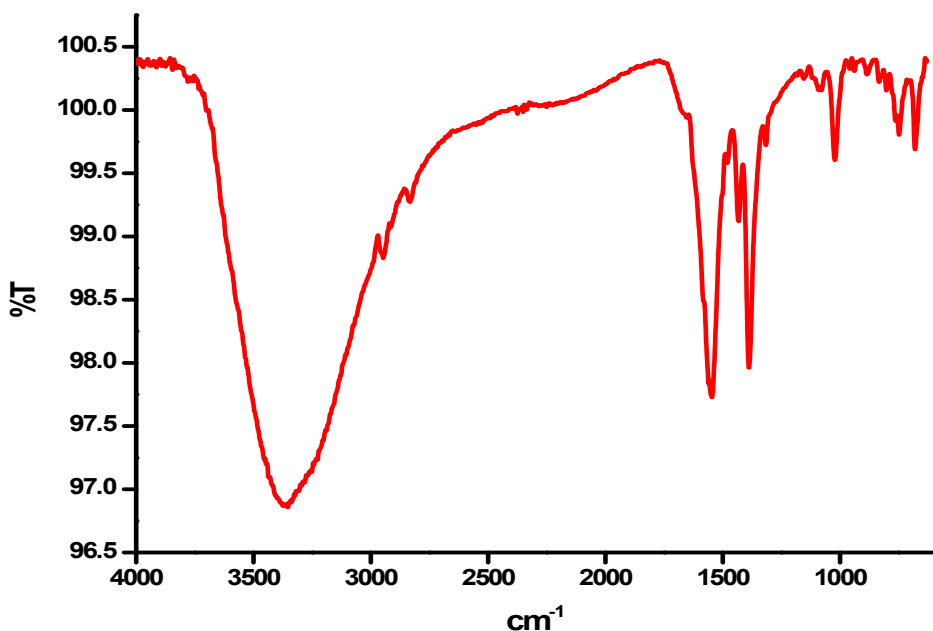


Figure S2. FTIR spectrum of **2-Ni**.

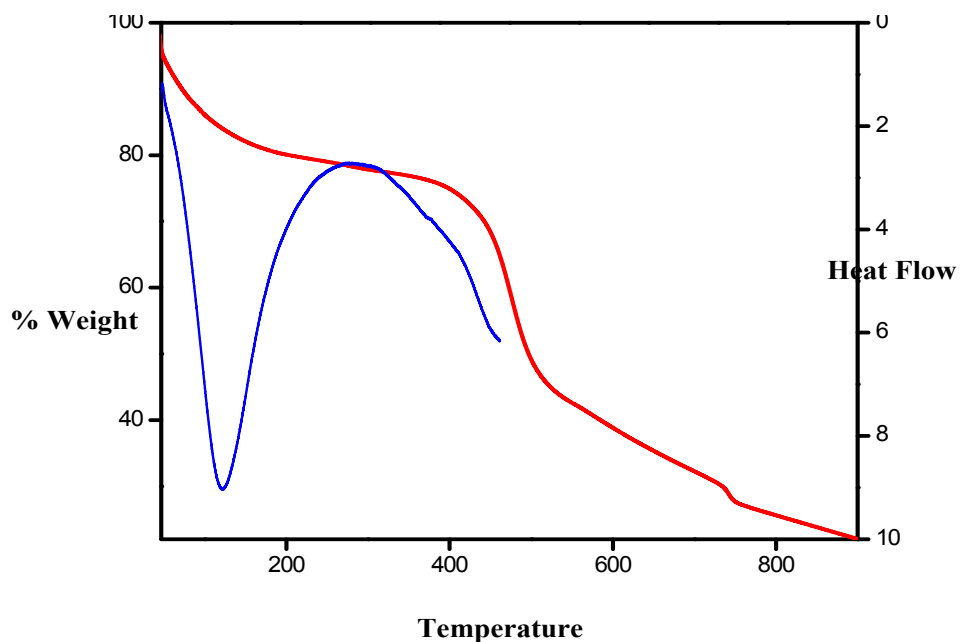


Figure S3. Thermal Gravimetric Analysis (TGA, red trace) and Differential Scanning Calorimetric (DSC, blue trace) plots for **1-Ni**.

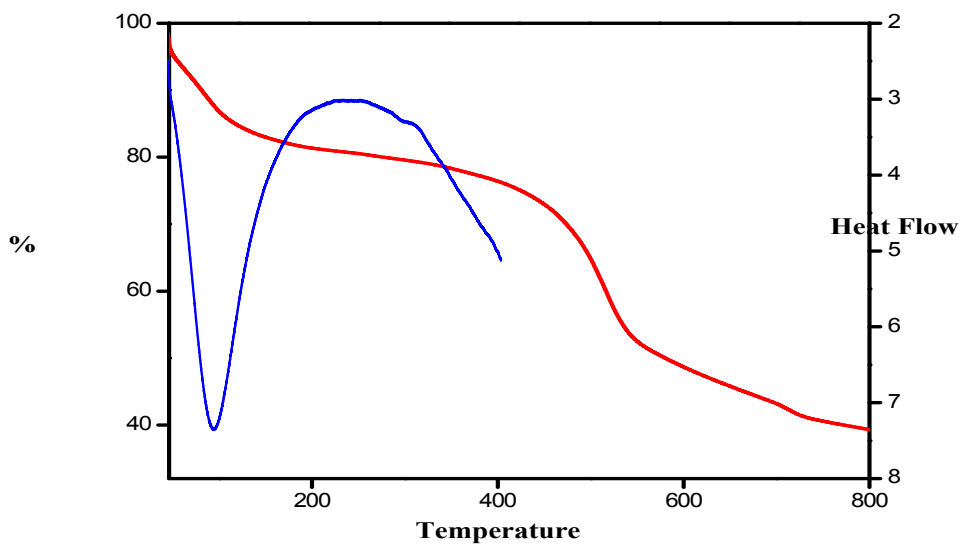


Figure S4. Thermal Gravimetric Analysis (TGA, red trace) and Differential Scanning Calorimetric (DSC, blue trace) plots for **2-Ni**.

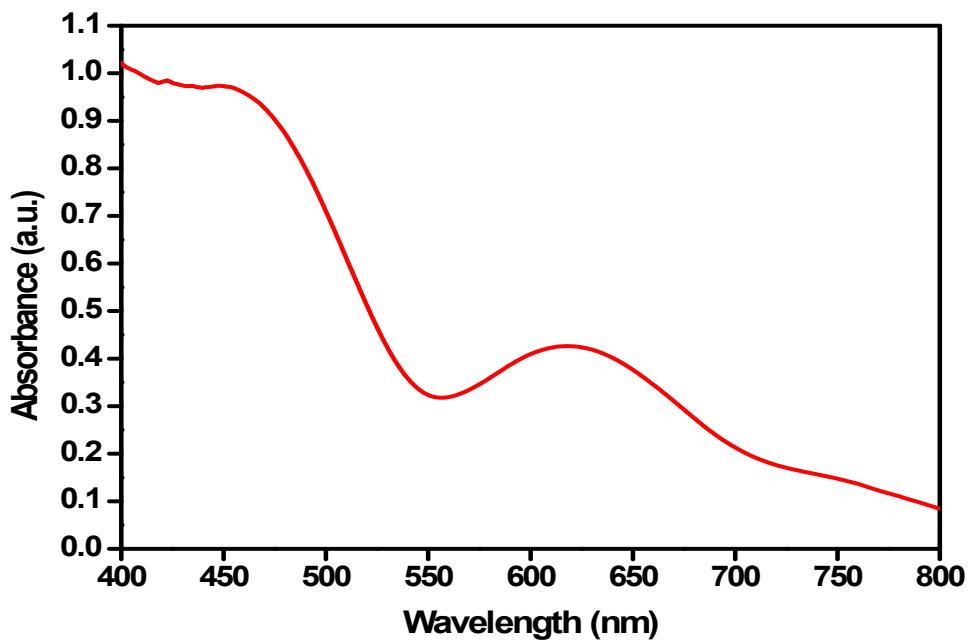


Figure S5. Diffuse reflectance UV-Vis spectrum of **1-Ni**.

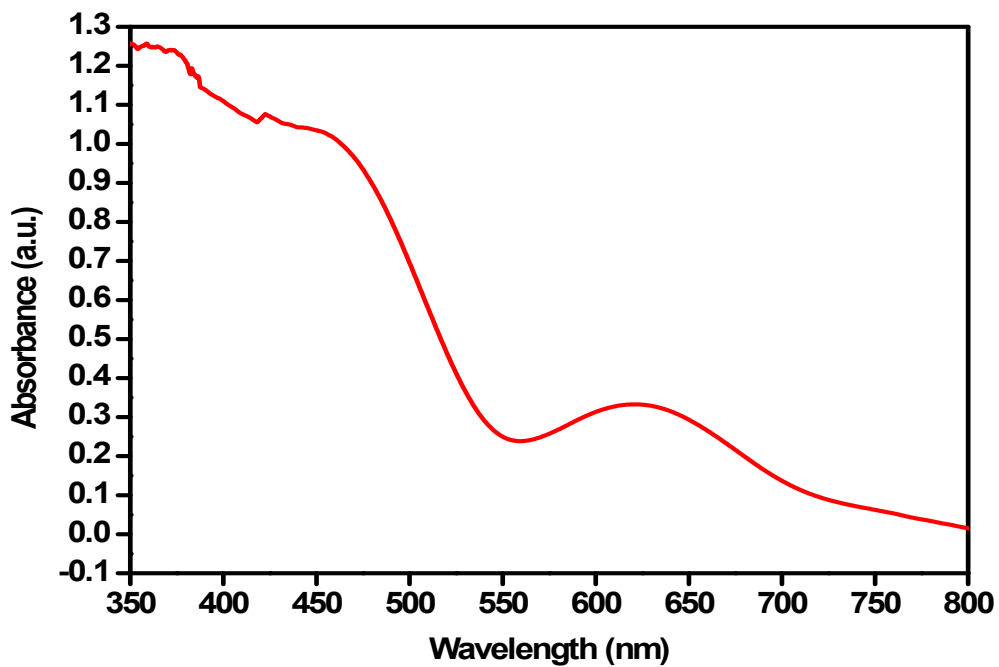


Figure S6. Diffuse reflectance UV-Vis spectrum of **2-Ni**.

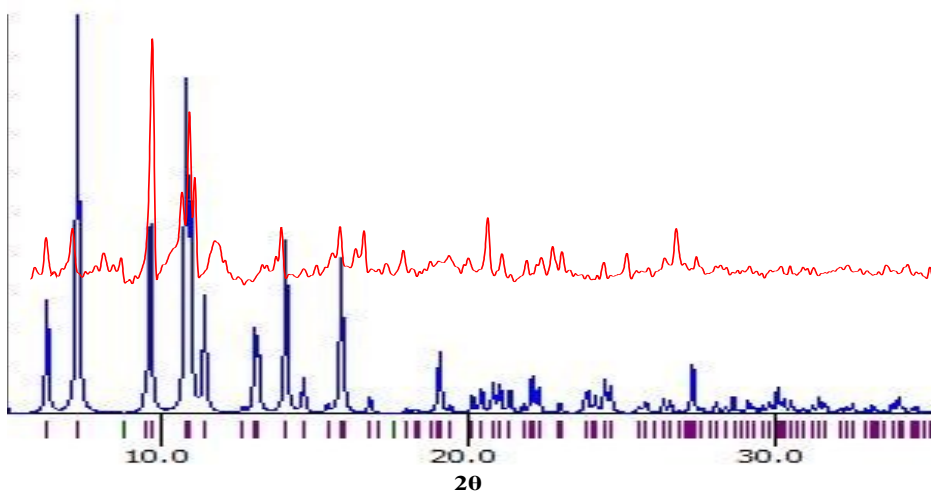


Figure S7. X-ray Powder Diffraction (XRPD) pattern for as-synthesized **1-Ni** (red trace) and the one simulated from the Mercury 3.8 using the single crystal data (blue trace).

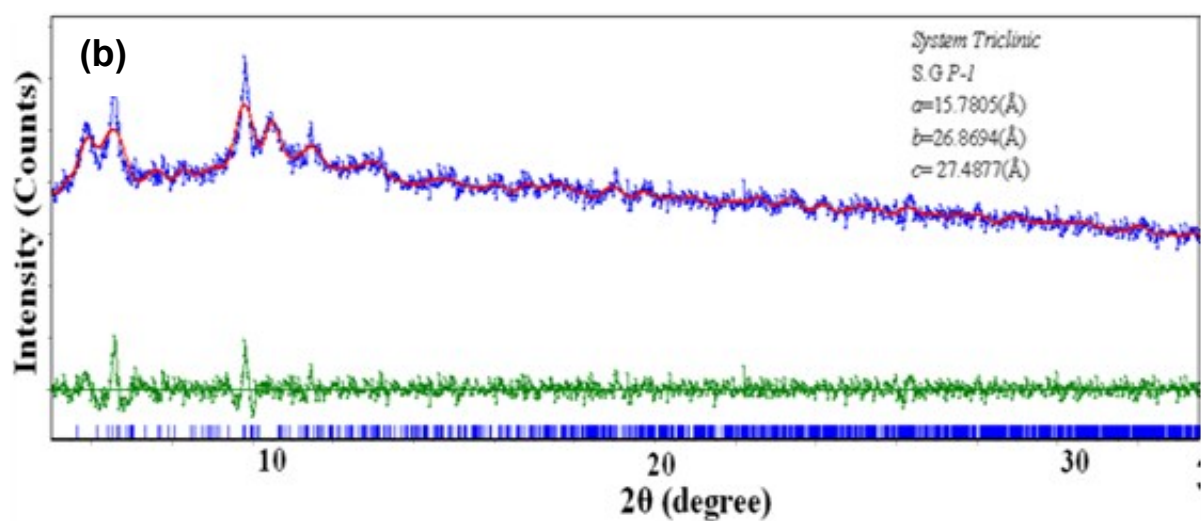
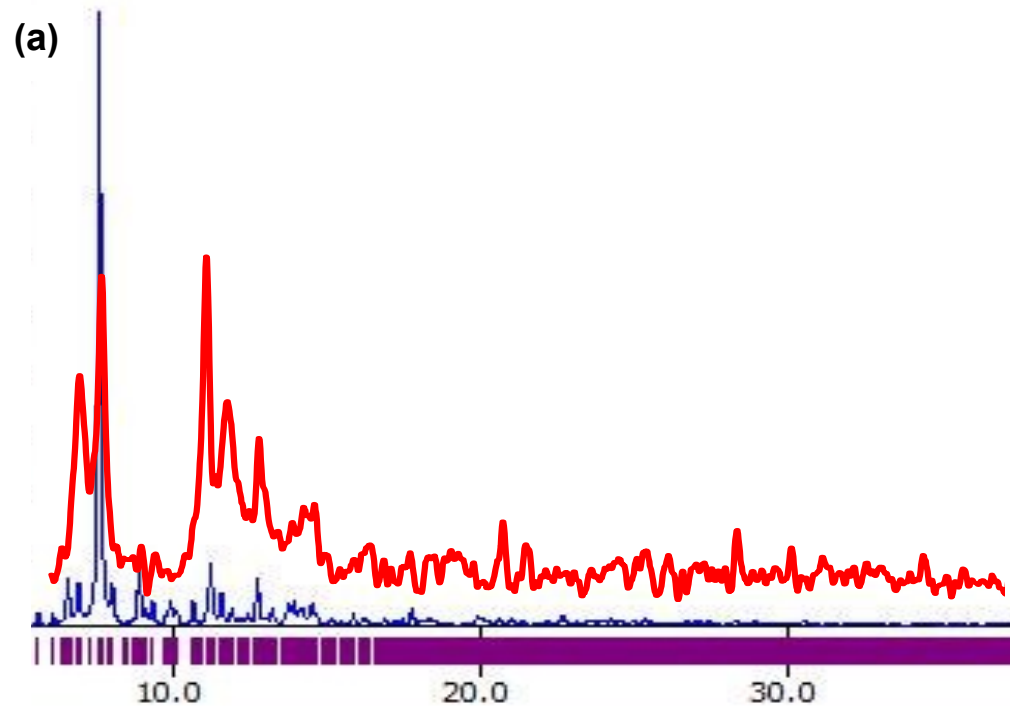


Figure S8. (a) X-ray Powder Diffraction (XRPD) pattern for as-synthesized **2-Ni** (red trace) and the one simulated from the Mercury 3.8 using the single crystal data (blue trace). (b) Le Bail refinement of XRPD pattern of **2-Ni**. The observed, calculated (profile matching), and difference profiles are given in blue, red, and olive lines, respectively. Generated Bragg positions are provided as blue vertical lines.

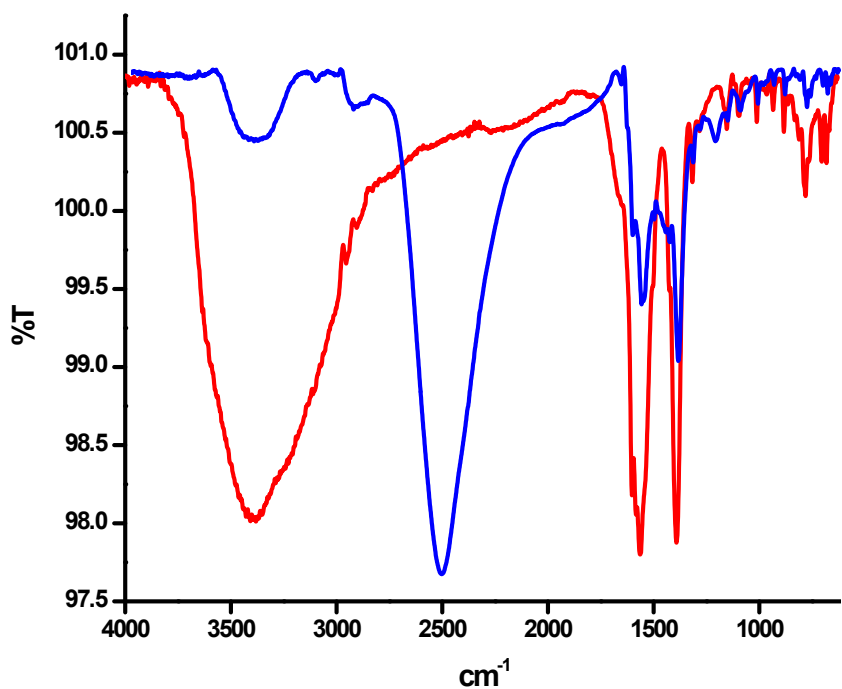


Figure S9. FTIR spectra of as synthesized **1-Ni** (red trace) and after  $\text{D}_2\text{O}$  exchange experiment (blue trace).

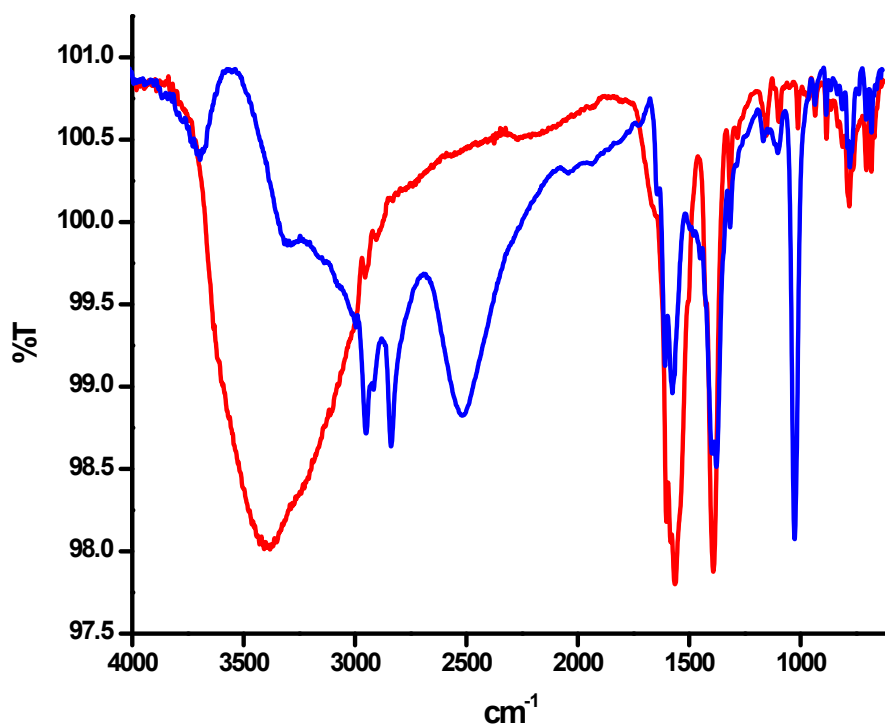


Figure S10. FTIR spectra of as synthesized **1-Ni** (red trace) and after  $\text{CH}_3\text{OH}$  exchange experiment (blue trace).

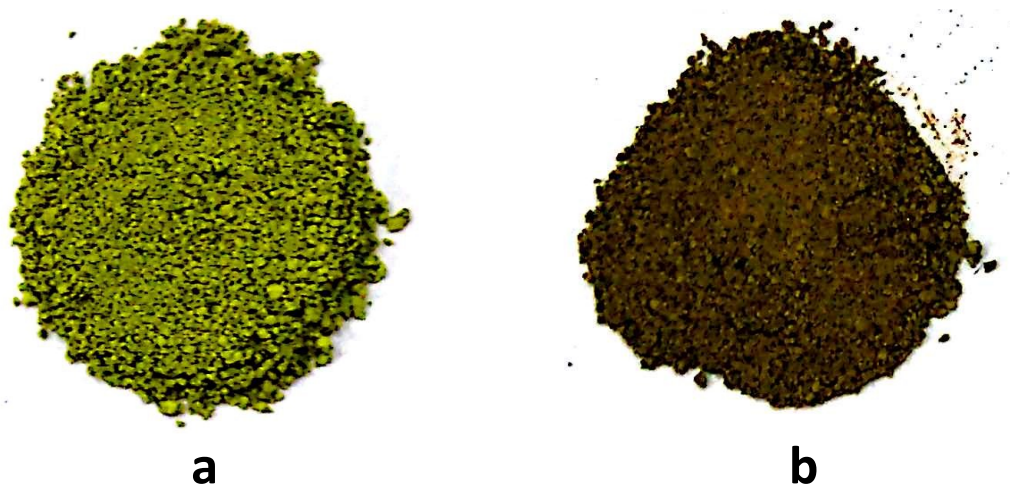


Figure S11. Optical images of a solid sample of (a) as synthesized **1-Ni** and after (b) iodine adsorption.

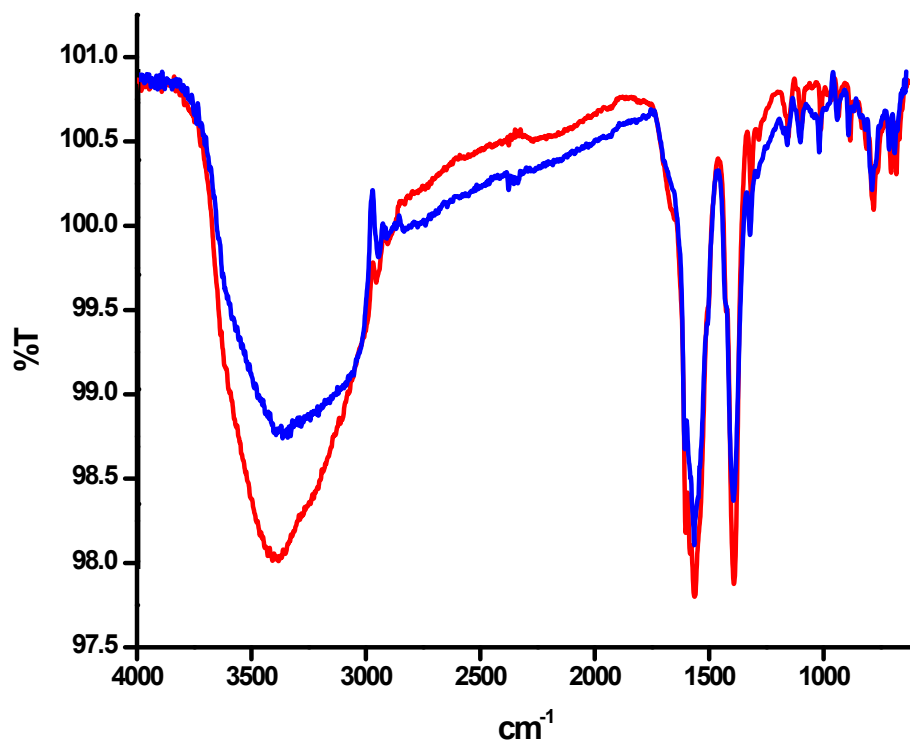


Figure S12. FTIR spectra of as synthesized **1-Ni** (red trace) and after C-S cross coupling reaction between 4-iodotoluene and thiophenol (blue trace).

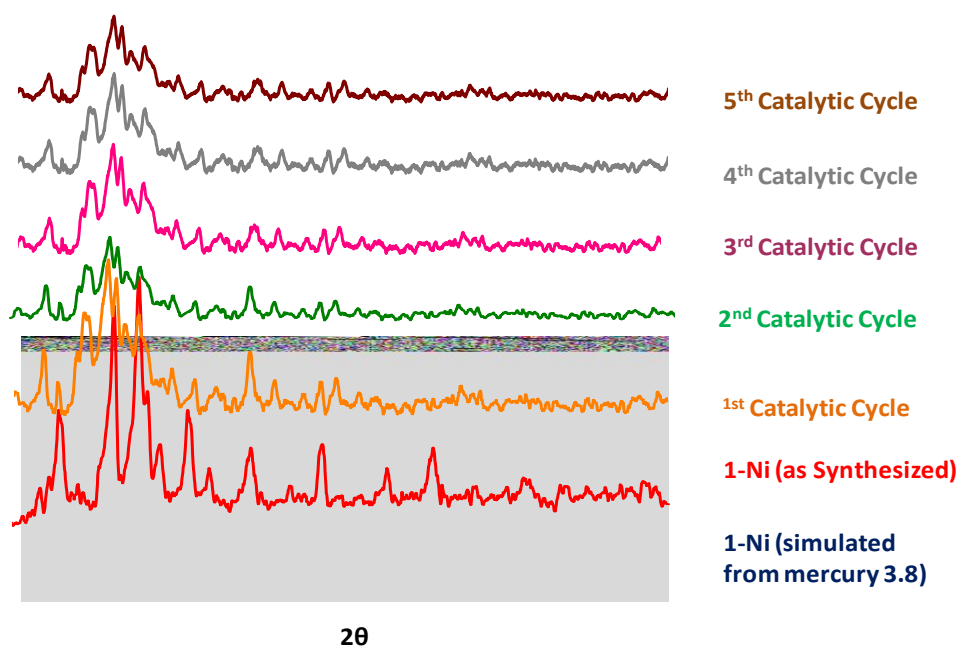


Figure S13. X-ray Powder Diffraction (XRPD) pattern for 1-Ni simulated from mercury 3.8 (blue trace), as synthesized **1-Ni** (red Trace) and after 5 cycles of C-S cross coupling reaction between 4-iodotoluene and thiophenol.

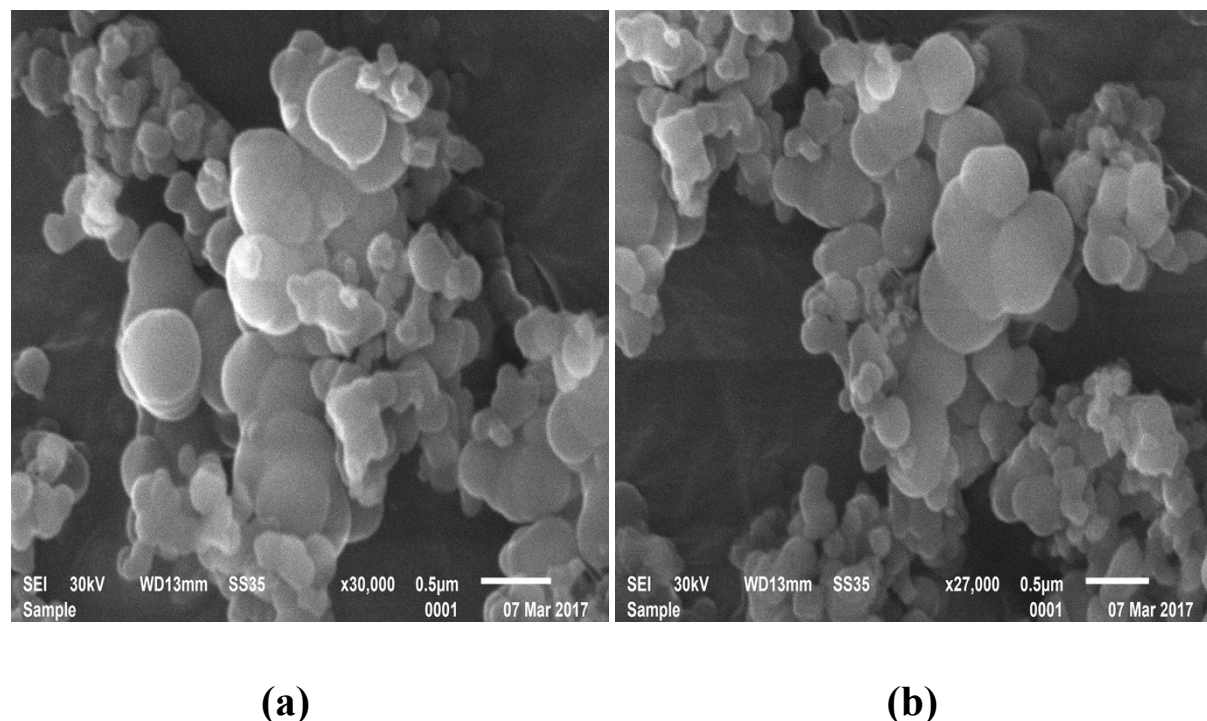


Figure S14. SEM images of as synthesized **1-Ni** (a) before and (b) after C-S cross coupling reaction between 4-iodotoluene and thiophenol.

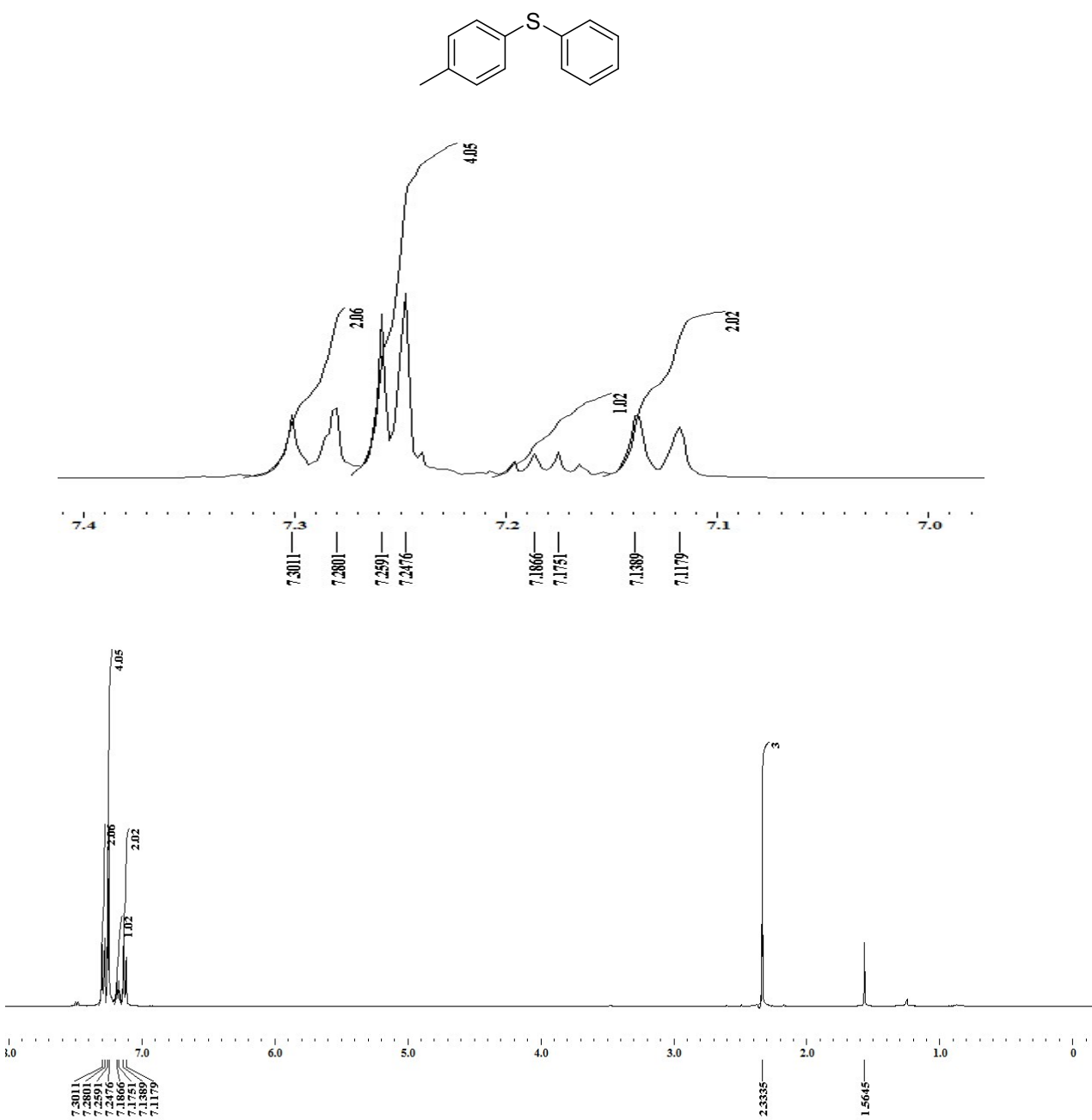


Figure S15.  $^1\text{H}$  NMR spectrum of phenyl(4-tolyl)sulfane in  $\text{CDCl}_3$ .

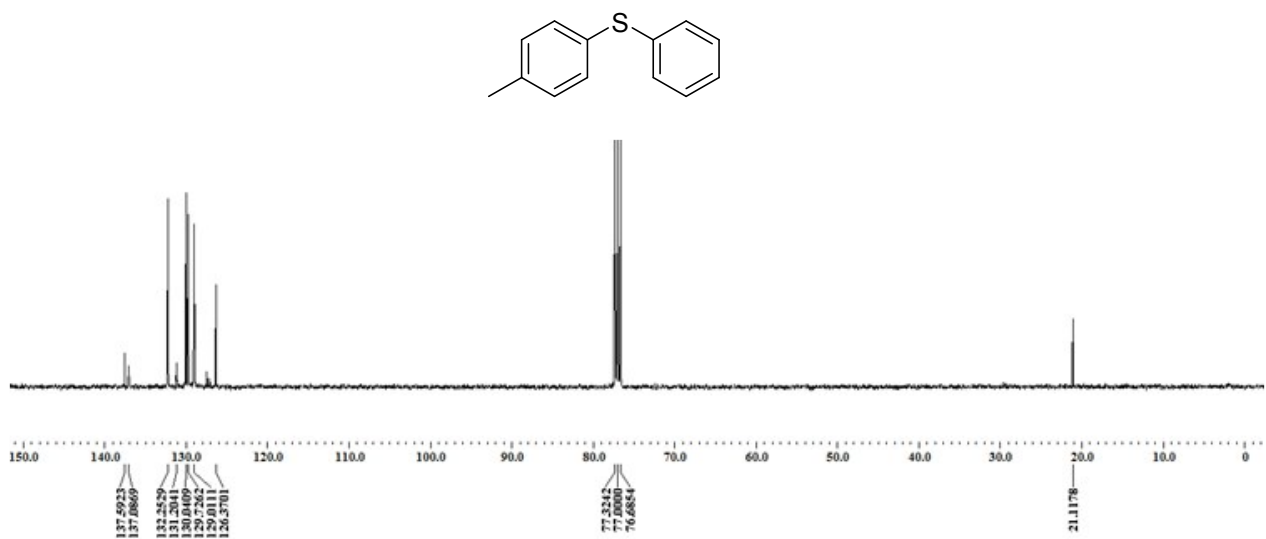


Figure S16.  $^{13}\text{C}$  NMR spectrum of phenyl(4-tolyl)sulfane in  $\text{CDCl}_3$ .

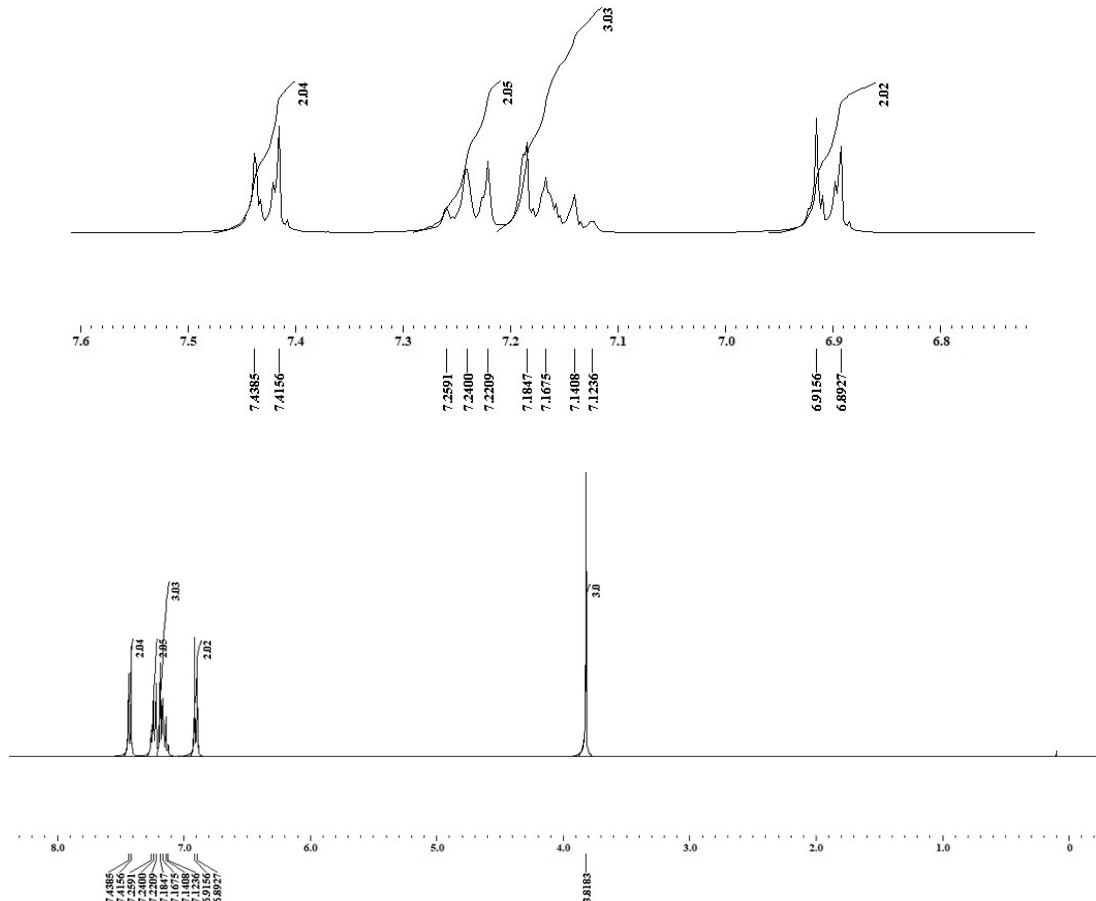
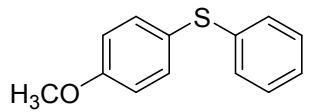


Figure S17. <sup>1</sup>H NMR spectrum of (4-methoxyphenyl)(phenyl)sulfane in CDCl<sub>3</sub>.

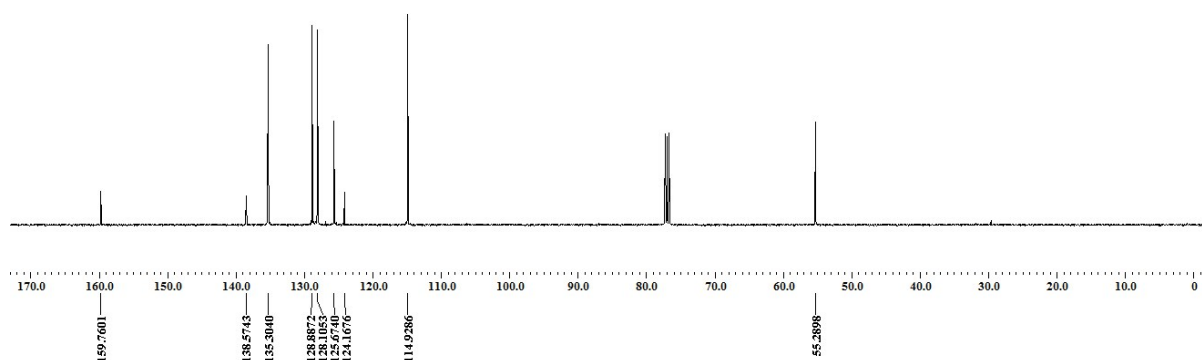
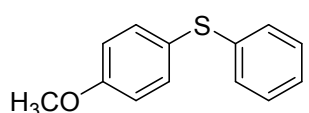


Figure S18. <sup>13</sup>C NMR spectrum of (4-methoxyphenyl)(phenyl)sulfane in CDCl<sub>3</sub>.

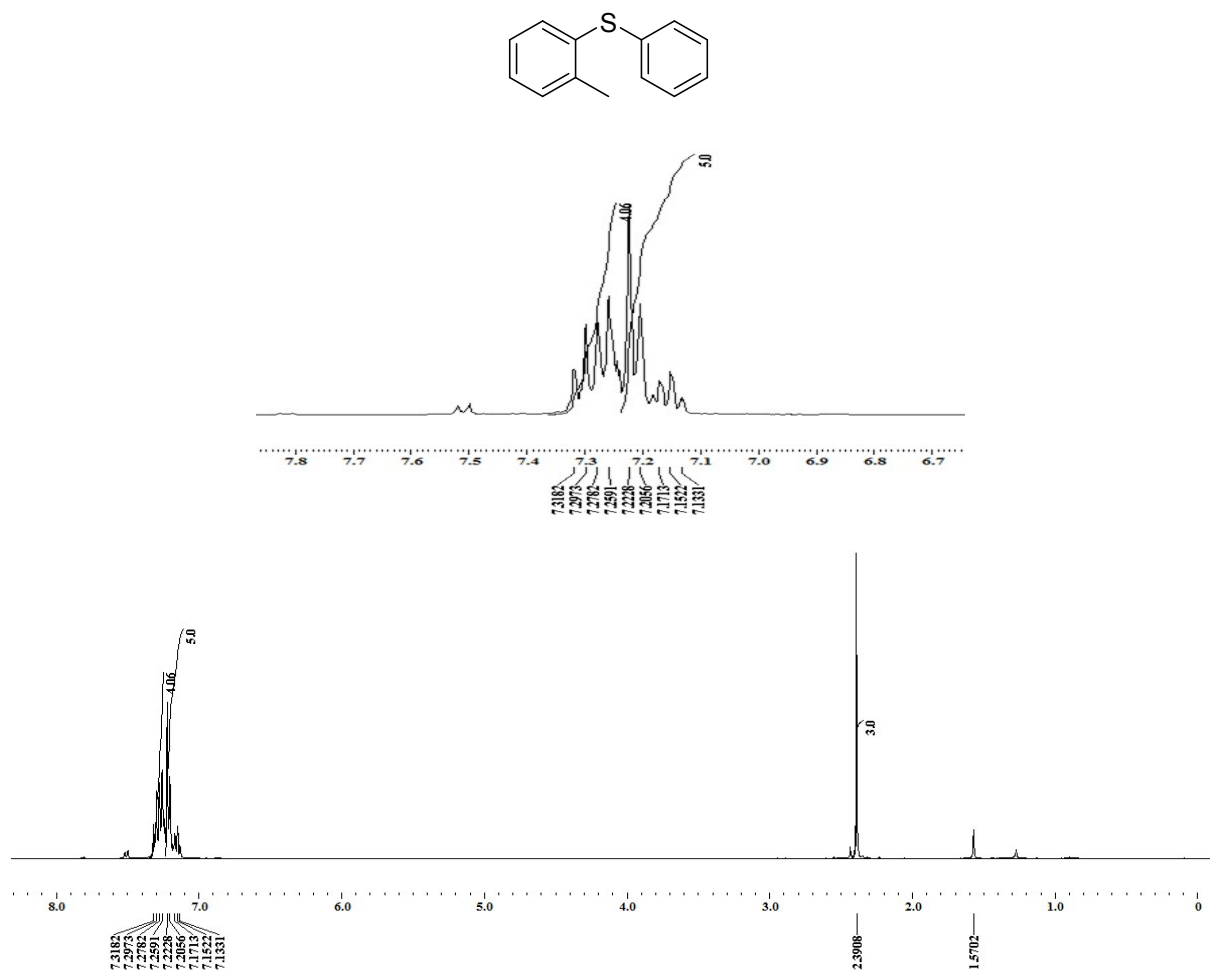


Figure S19.  $^1\text{H}$  NMR spectrum of phenyl(2-tolyl)sulfane in  $\text{CDCl}_3$ .

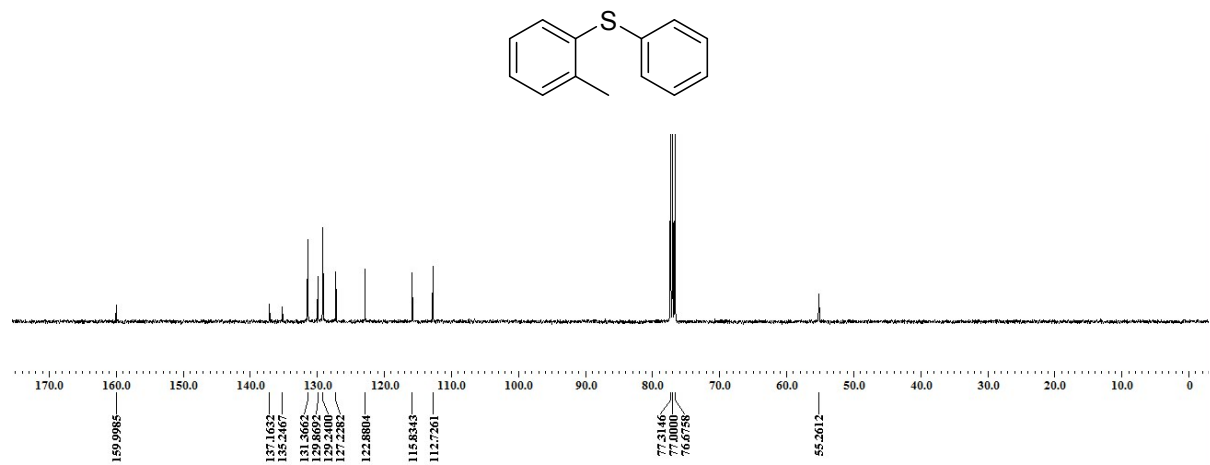


Figure S20.  $^{13}\text{C}$  NMR spectrum of phenyl(2-tolyl)sulfane in  $\text{CDCl}_3$ .

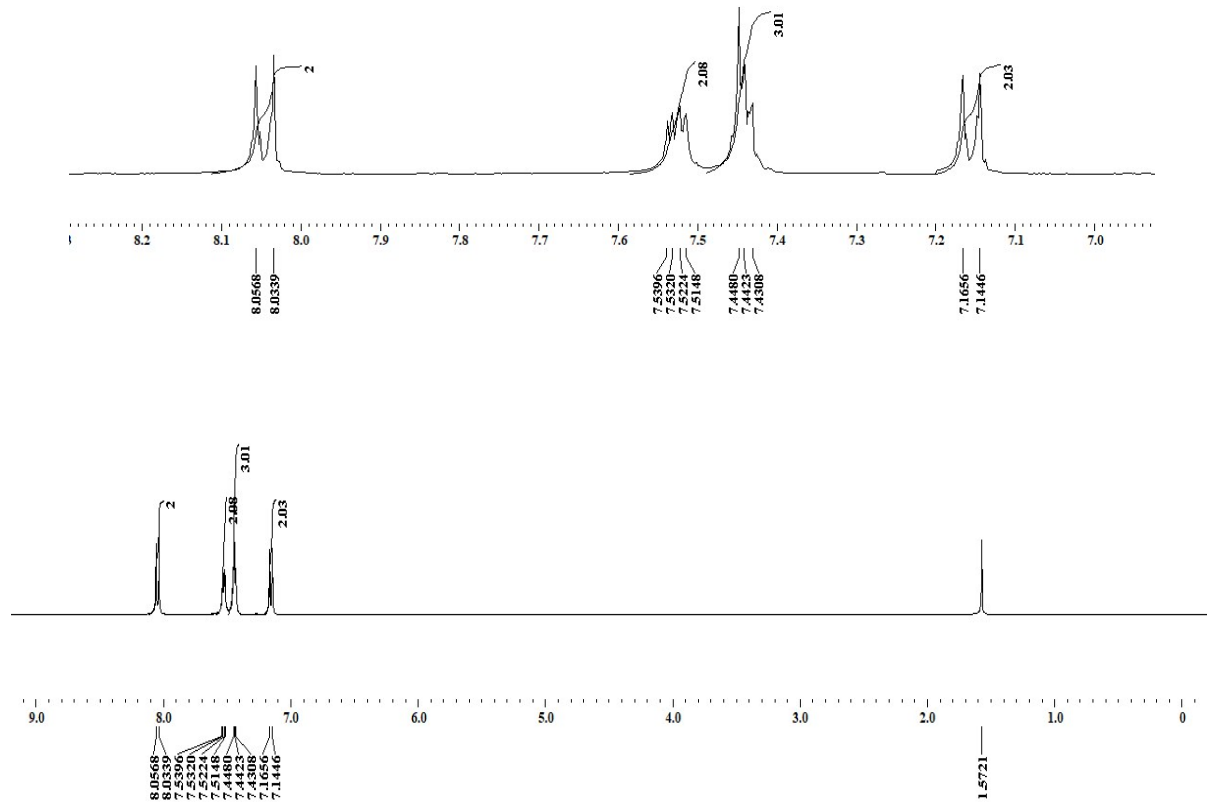
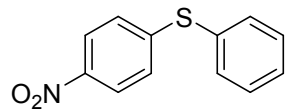


Figure S21.  $^1\text{H}$  NMR spectrum of (4-nitrophenyl)(phenyl)sulfane in  $\text{CDCl}_3$ .

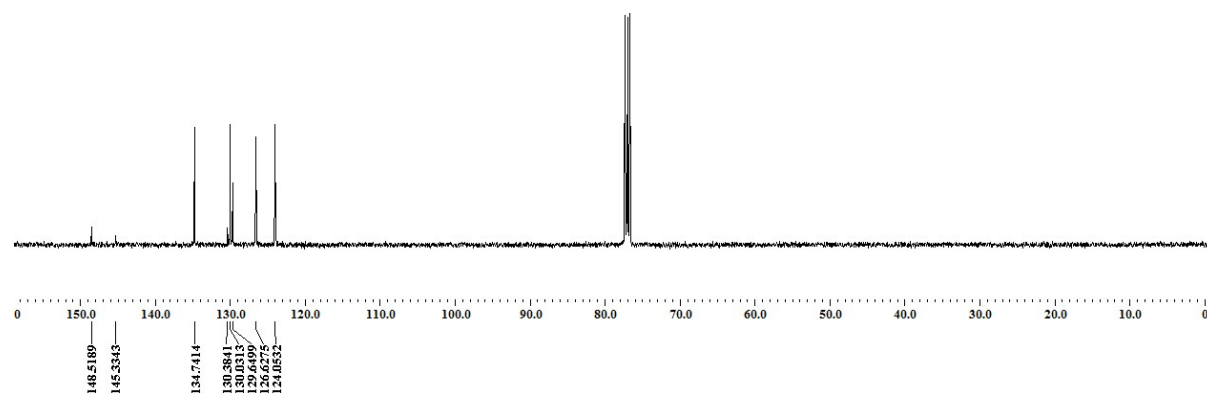
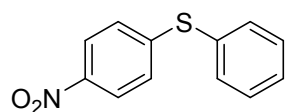


Figure S22.  $^{13}\text{C}$  NMR spectrum of (4-nitrophenyl)(phenyl)sulfane in  $\text{CDCl}_3$ .

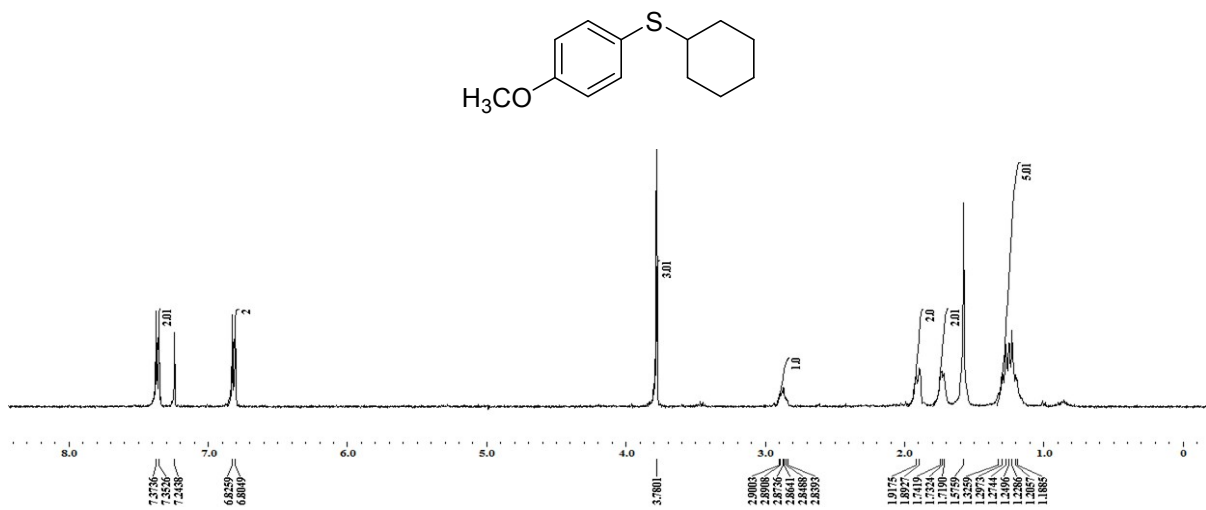


Figure S23.  $^1\text{H}$  NMR spectrum of cyclohexyl(4-methoxyphenyl)sulfane in  $\text{CDCl}_3$ .

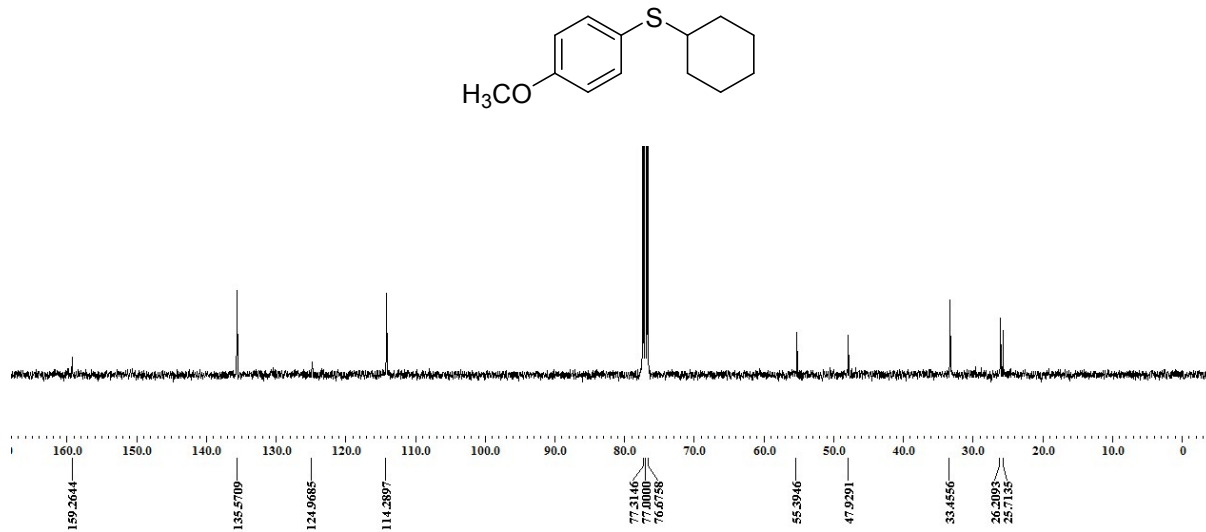


Figure S24.  $^{13}\text{C}$  NMR spectrum of cyclohexyl(4-methoxyphenyl)sulfane in  $\text{CDCl}_3$ .

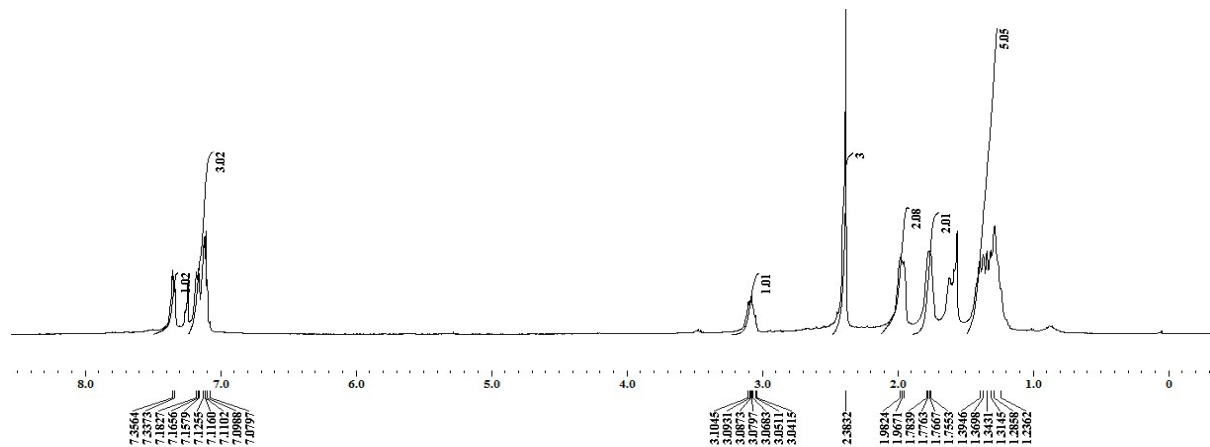
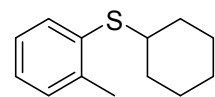


Figure S25.  $^1\text{H}$  NMR spectrum of cyclohexyl(2-tolyl)sulfane in  $\text{CDCl}_3$ .

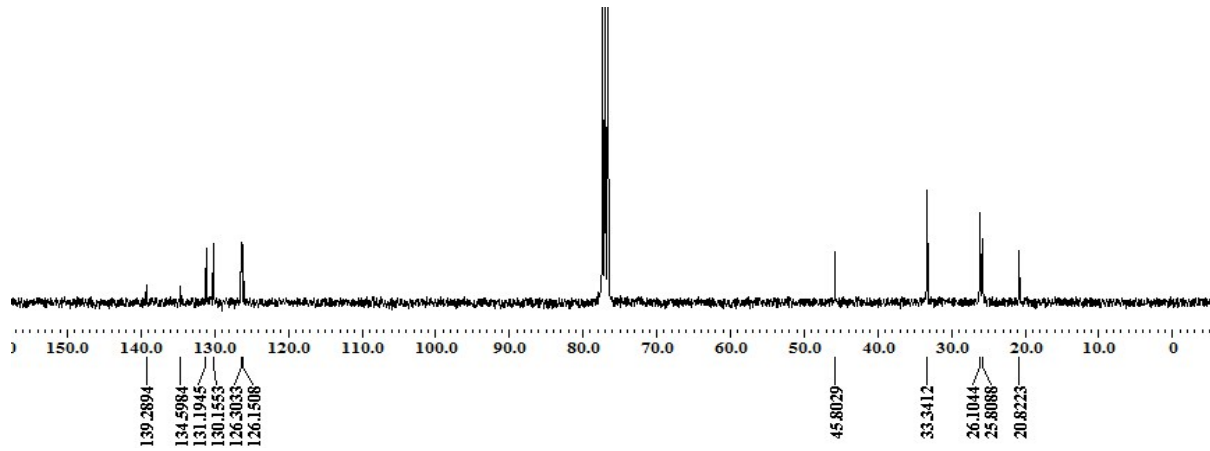
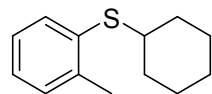


Figure S26.  $^{13}\text{C}$  NMR spectrum of cyclohexyl(2-tolyl)sulfane in  $\text{CDCl}_3$ .

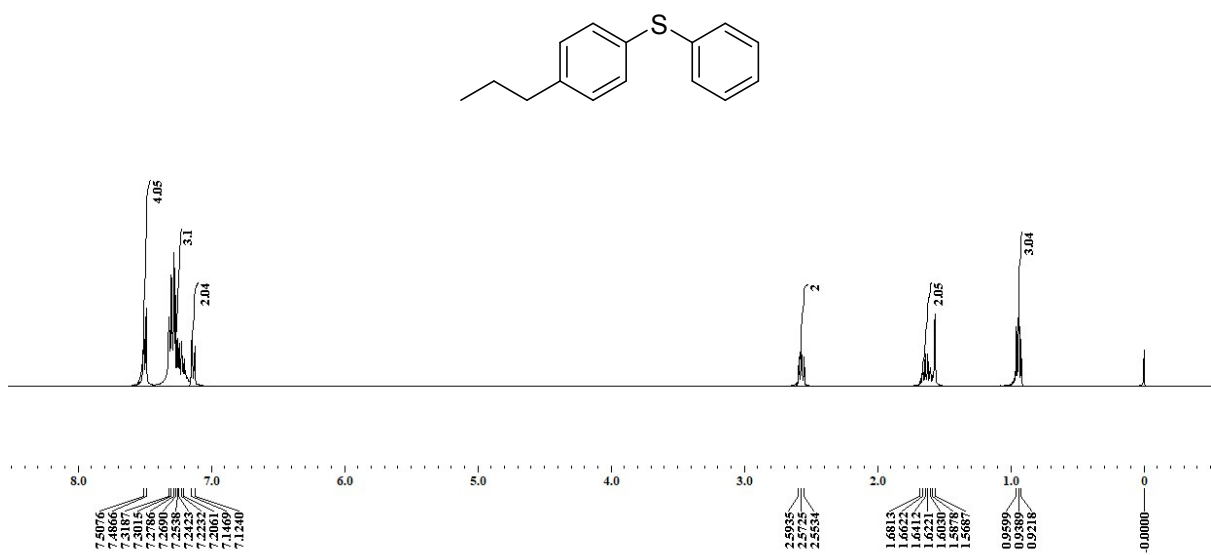


Figure S27.  $^1\text{H}$  NMR spectrum of phenyl(4-propylphenyl)sulfane in  $\text{CDCl}_3$ .

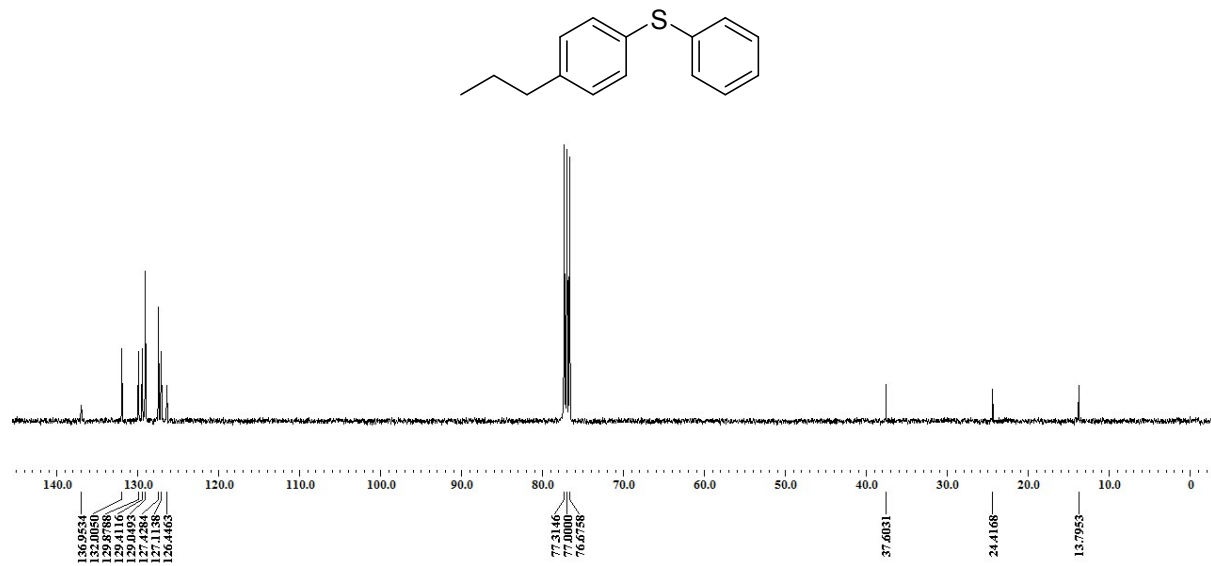


Figure S28.  $^{13}\text{C}$  NMR spectrum of phenyl(4-propylphenyl)sulfane in  $\text{CDCl}_3$ .

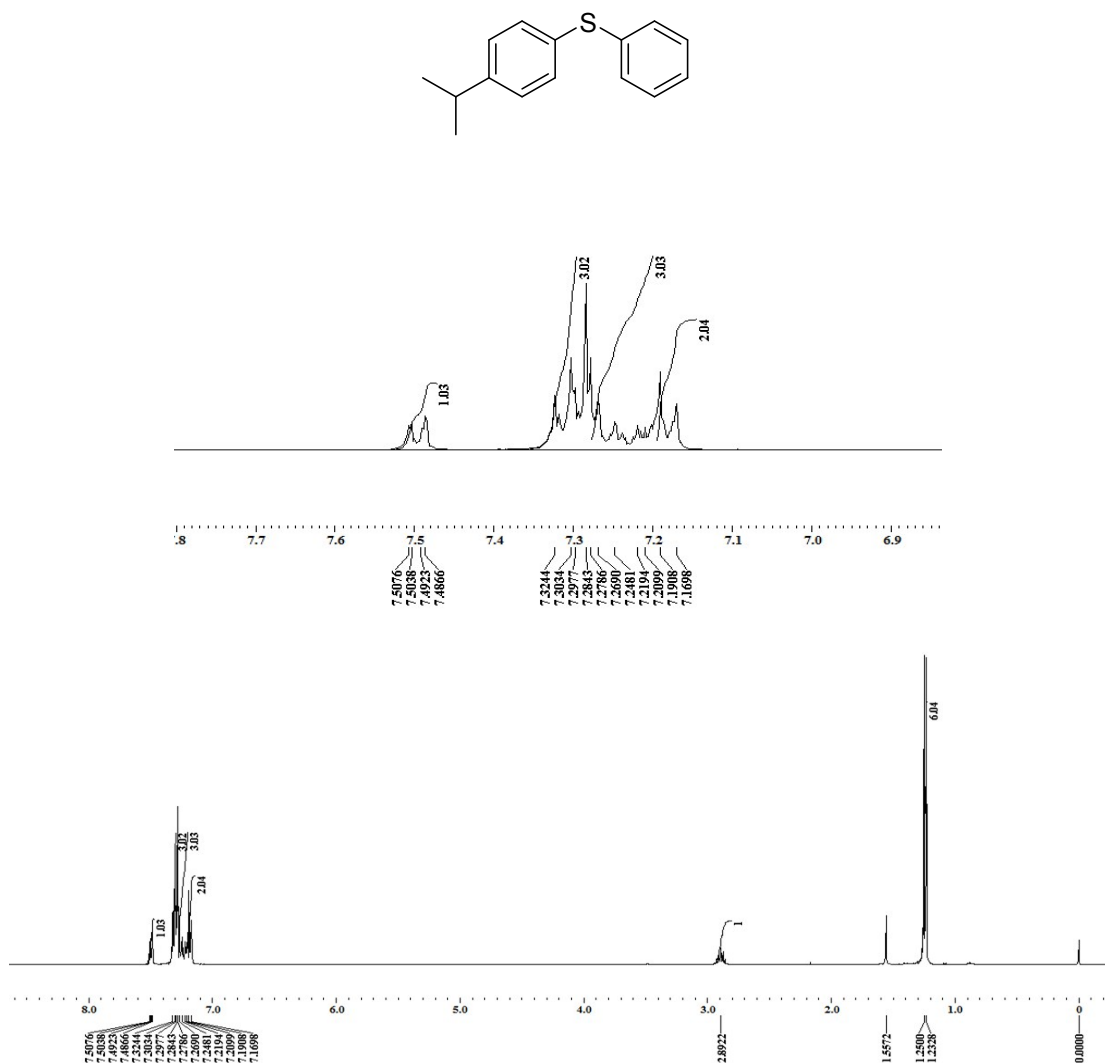


Figure S29.  $^1\text{H}$  NMR spectrum of (4-isopropylphenyl)(phenyl)sulfane in CDCl<sub>3</sub>.

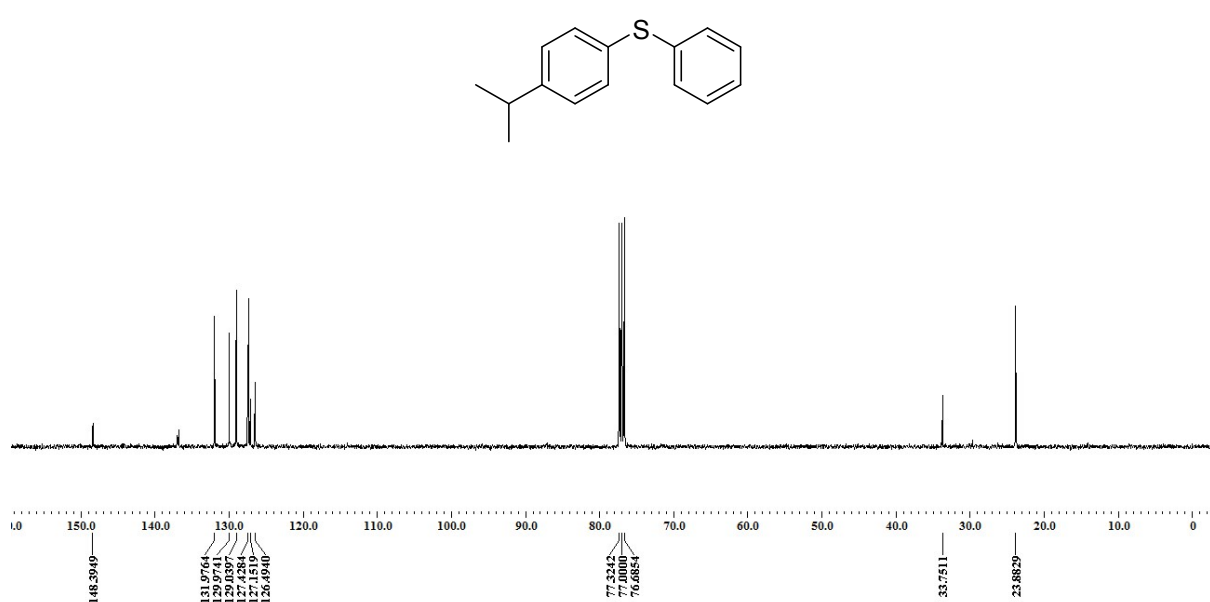


Figure S30.  $^{13}\text{C}$  NMR spectrum of (4-isopropylphenyl)(phenyl)sulfane in CDCl<sub>3</sub>.

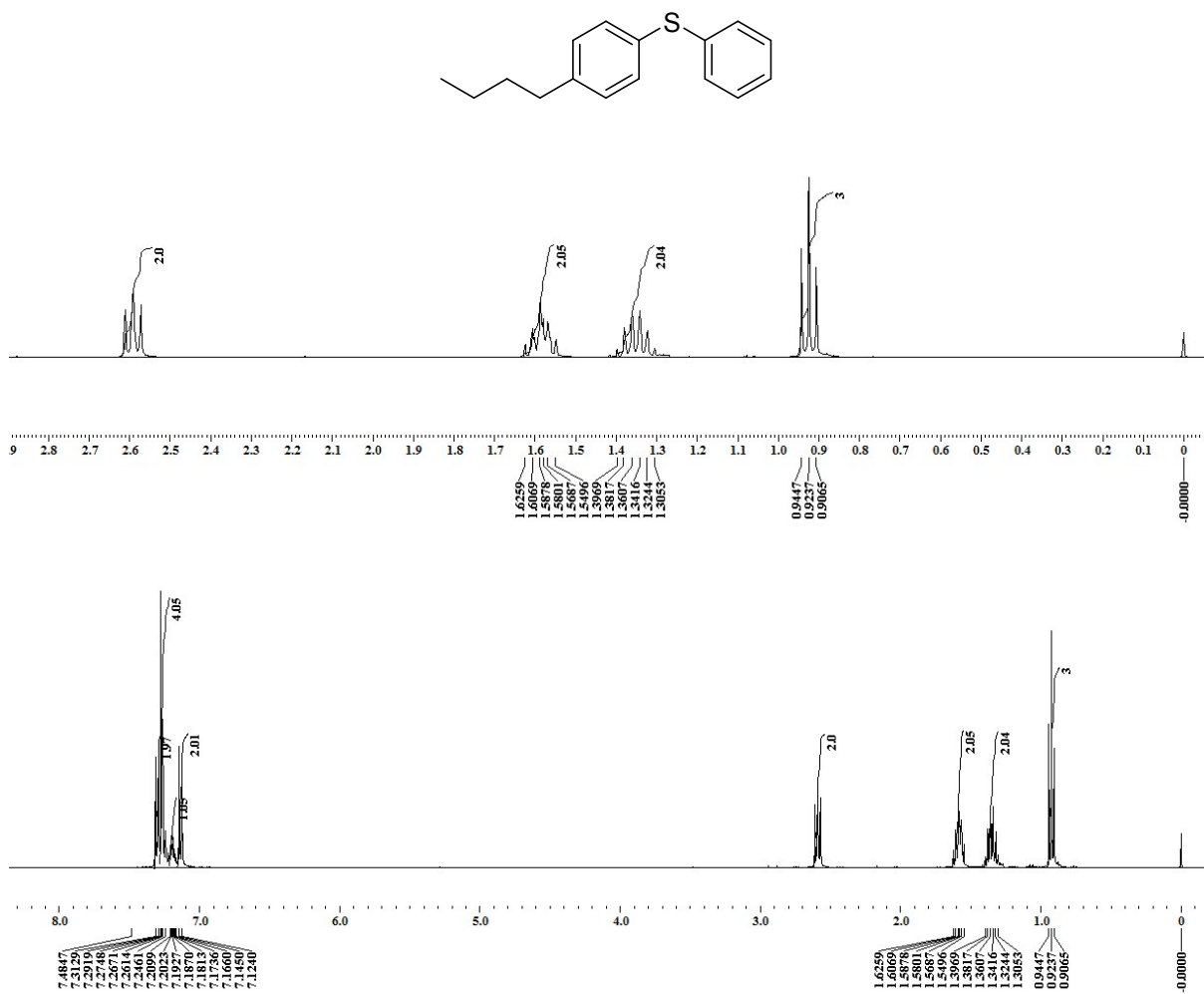


Figure S31. <sup>1</sup>H NMR spectrum of (4-butylphenyl)(phenyl)sulfane in CDCl<sub>3</sub>.

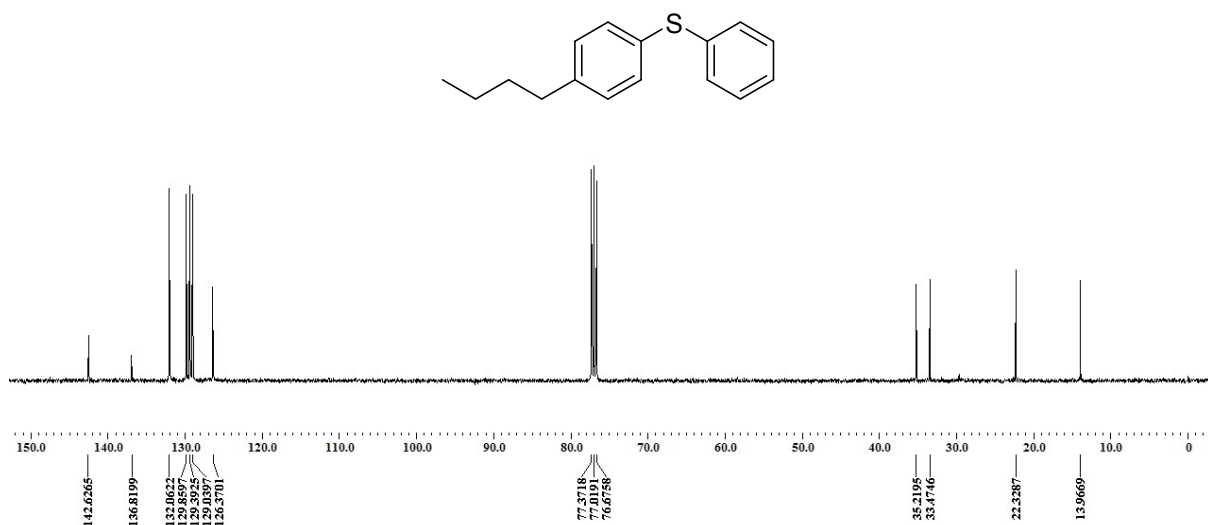


Figure S32. <sup>13</sup>C NMR spectrum of (4-butylphenyl)(phenyl)sulfane in CDCl<sub>3</sub>.

Table S1. Crystallographic data collection and structural refinement parameters for **1-Ni**.

<b>1</b>	<b>1-Ni</b>
Empirical formula	C <sub>42</sub> H <sub>46</sub> CoN <sub>6</sub> Ni <sub>2</sub> O <sub>24</sub>
Formula weight	1195.20
T(K)	173(2)
Crystal system	Hexagonal
Space group	P 6 <sub>2</sub> 2 2
<i>a</i> (Å)	27.857(2)
<i>b</i> (Å)	27.857(2)
<i>c</i> (Å)	10.0365(7)
$\alpha(^{\circ})$	90
$\beta(^{\circ})$	90
$\gamma(^{\circ})$	120
<i>V</i> (Å) <sup>3</sup>	6745.2(11)
<i>Z</i>	3
Crystal Size (mm <sup>3</sup> )	0.2 x 0.15 x 0.12
<i>d</i> [g cm <sup>-3</sup> ]	0.883
$\mu$ [mm <sup>-1</sup> ]	0.648
<i>F</i> (000)	1845.0
<i>R</i> (int.)	0.1768
Final <i>R</i> indices <sup>a</sup>	R1 = 0.0543
[ <i>I</i> >2σ( <i>I</i> )]	wR2 = 0.0995
<i>R</i> indices	R1 = 0.0712
All data	wR2 = 0.1054
GOF on <i>F</i> <sup>2</sup>	0.944
CCDC No.	

$$R_1 = \frac{\sum ||F_o - |F_c||}{\sum |F_o|}, \quad wR_2 = \left\{ \frac{\sum [w(|F_o|^2 - |F_c|^2)^2]}{\sum [wF_o^4]} \right\}^{1/2}$$